



# Precise determination of energy transfer upconversion coefficient for the erbium and ytterbium codoped laser crystals

YUANJI LI,<sup>1,2</sup> KUNLUN LIU,<sup>1</sup> JINXIA FENG,<sup>1,2</sup> YUJIN CHEN,<sup>3</sup>  
YIDONG HUANG,<sup>3</sup> AND KUANSHOU ZHANG<sup>1,2,\*</sup>

<sup>1</sup>State Key Laboratory of Quantum Optics and Quantum Optics Devices, Institute of Opto-Electronics, Shanxi University, Taiyuan 030006, China

<sup>2</sup>Collaborative Innovation Center of extreme Optics, Shanxi University, Taiyuan 030006, China

<sup>3</sup>Key Laboratory of Optoelectronic Materials Chemistry and Physics, Fujian Institute of Research on the Structure of Matter, Chinese Academy of Sciences, Fuzhou, Fujian 350002, China

\*kuanshou@sxu.edu.cn

**Abstract:** Energy transfer upconversion (ETU) coefficient plays a crucial role in investigating complex laser systems as it greatly influences both the laser output behavior and heat generation. For some quasi-three-energy-level lasers based on Er<sup>3+</sup> doped, Ho<sup>3+</sup> doped and codoped gain media, the available theoretical studies relied on some unreasonable approximations due to the lack of spectroscopic data, notably the ETU coefficient. We put forward what we believe is a novel approach to overcome the difficulties caused by wavelength jump occurred in aforementioned laser systems. Based on net gain cross-section analysis and rate equations modelling, the functional relationship between the ETU coefficient, the laser power and pump power at the jumping wavelength are established. ETU coefficients and their temperature dependences of Er,Yb:YAB crystals with different crystal doped concentrations are experimentally determined for the first time. The results reveal that the ETU process in Er,Yb:YAB laser system is 5~35 times stronger than that in Er<sup>3+</sup> and Yb<sup>3+</sup> codoped phosphate glass. The determination of these spectroscopic data paves the way for precise modelling of laser system based on Er,Yb:YAB or similar gain media.

© 2023 Optica Publishing Group under the terms of the [Optica Open Access Publishing Agreement](#)

## 1. Introduction

Spectroscopic parameters of laser gain media, for instance energy transfer upconversion (ETU) coefficient, play an important role in the laser behaviors of either the strongly pumped four-energy-level lasers or the quasi-three-energy-level lasers [1–5]. Generally, ETU process not only depletes the inversion population and consequently lowers the laser efficiency, but also raises up the thermal load inside the gain media. Therefore, measurement of the ETU coefficient and the studies on the relations between ETU coefficient and other parameters are of great value for understanding the laser behaviors and providing guidance to laser optimization.

To date, there are mainly three methods for the experimental determination of ETU coefficient. The spectroscopic method in the outset was based on the resonant energy transfer (RET) theory proposed by T. Förster and D. L. Dexter [6,7]. Quantitative characterization of ETU can be achieved by RET theory using the microparameters of energy transfer and migration, indicated by  $C_{DA}$  and  $C_{DD}$ , which can be evaluated based on the emission spectra of the donor and the absorption spectra of both the donor and acceptor [6]. Nevertheless, spectroscopic method in recent investigations were relied on fluorescence detection and rate equation modelling [8,9]. With short pulse laser pumping, N. P. Barnes et al. predicted the ETU coefficient of Er:YAG by measuring the rise and decay of the fluorescence intensity related to the meta-stable energy level involved in ETU, and fitting the data with the rate equations model [8]. However, one

may note that the results obtained from the method showed nonnegligible relative error and multiple outliers, especially at the case of low doped concentration, which may be due to the limited precision in fluorescence detection and fitting process, temperature variation under dense pumping and the disturbance stem from stimulated emission existed in the pumped crystal powder. The second method named as z-scan was based on pump absorption measurements along the z-direction, i.e. the pump laser propagation direction, inside the crystal at various pump intensities, since the implications of ETU on the change of ground state population was directly related to the pump laser absorption inside the gain medium [10,11]. Good measurement accuracy had been realized by z-scan for a series of four-energy-level lasers including Nd:YVO<sub>4</sub> lasers and Nd:YLF lasers. Note that high measurement accuracy could only be guaranteed when the power stability and beam quality of the pump laser were both extremely well. Ultimately though, this method had never been utilized for lasers based on Er<sup>3+</sup> doped, Ho<sup>3+</sup> doped or Er<sup>3+</sup> and Yb<sup>3+</sup> codoped gain media, which were usually named as quasi-three-energy-level systems, for the reason that the relationship between the ETU coefficient and pump transmission in this kind of lasers became quite complicate unless significant simplifications were made. The third method was relied on the analysis of ETU dependence of the laser threshold [12,13]. When the laser thresholds at various laser intracavity loss, usually varied by changing the output coupling transmission, was recorded experimentally, the ETU coefficient was then fitted with a rate equation model. Comparing with the previous two methods, this method exhibited the advantages of simple configuration and low cost. However, for the Er<sup>3+</sup> doped, Er<sup>3+</sup> and Yb<sup>3+</sup> codoped, and Ho<sup>3+</sup> doped quasi-three-energy-level laser systems, the laser threshold was known depending on the oscillation wavelength, hence the method was incapable to deal with the wavelength jump phenomena when intracavity loss was tuned [14–21].

In this paper, a new method for measuring ETU coefficient in quasi-three-energy-level laser systems was proposed. The function relationship between ETU coefficient, the jumping oscillation wavelength, the pump power and laser power when the wavelength jump occurred was derived on the basis of a model involving net gain cross-section spectra analysis and rate equations. By constructing continuous wave single frequency solid-state lasers (CWSFLs) based on Er,Yb:YAB crystal with different doped concentrations, the ETU coefficient, as well as its temperature and doped concentration dependences were determined utilizing the model and laser output parameters.

## 2. Mechanism of wavelength variation for 1.5 μm CWSFL depending on the energy transfer upconversion

Considering the dispersive behavior of intracavity loss ( $\delta_t(\lambda)$ ), net gain cross-section of a Er,Yb:YAB laser can be defined as [22–25]

$$G(\lambda) = N_E l [\beta \sigma_{em}(\lambda) - (1 - \beta) \sigma_{abs}(\lambda)] / n - \delta_t(\lambda), \quad (1)$$

where  $N_E$  is the population density of Er<sup>3+</sup> ions,  $l$  is the length of the gain medium,  $\beta$  is the inversion fraction factor, indicating the ratio of the excited Er<sup>3+</sup> ions number to the total number of Er<sup>3+</sup> ions,  $\sigma_{abs}$  and  $\sigma_{em}$  are the stimulated absorption cross-section and the stimulated emission cross-section for the gain medium which are assumed to be invariant when the crystal temperature is varied in a relative small range,  $n$  is the refractive index of gain medium.

Using Eq. (1) and the cross-section spectra of an Er(1.1 at.%),Yb(25 at.%):YAB crystal, simulations can be carried out with following parameter values:  $N_E = 5.96 \times 10^{25} \text{ m}^{-3}$ ,  $l = 1 \text{ mm}$ ,  $n = 1.7508$ , while  $\delta_t(\lambda)$  is obtained using the dispersive transmission data of the coatings on the cavity mirrors and sapphire plates (see Supplement 1). As shown in Fig. 1, the lineshape of the net gain cross-section spectra is significantly affected by the value of  $\beta$ , leading to a varied wavelength corresponding to the peak of the spectra. Since this wavelength has the highest

probability to be oscillated owing to the mode competition, one can find that the predicted oscillating wavelength ( $\lambda_{osc}$ ) is changed non-uniformly with increasing  $\beta$ .

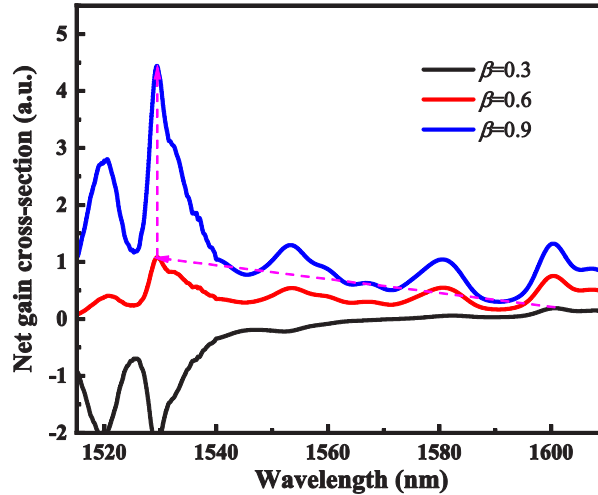


**Fig. 1.** Net gain cross-section of an Er(1.1 at.%), Yb(25 at.%):YAB crystal as a function of wavelength.

More specifically, when the computation was repeated in a loop that the value of  $\beta$  was varied from 0.01 to 1, the net gain cross-section spectrum was simulated at each given value of  $\beta$ , and the oscillating wavelength  $\lambda_{osc}$  was predicted using a peak search program (see Supplement 1). One can find that the  $\lambda_{osc}$  versus  $\beta$  curve shows a multi-step shape. For an Er(1.1 at.%), Yb(25 at.%):YAB crystal, as shown in Fig. 2(a), there are three critical values of  $\beta$ , namely  $\beta=0.14$ ,  $\beta=0.24$  and  $\beta=0.57$ , at the case of  $\beta=0.14$ ,  $\lambda_{osc}$  jumps from 1591 nm to 1610 nm, at  $\beta=0.24$ ,  $\lambda_{osc}$  jumps from 1610 nm to 1600 nm, and at the third case ( $\beta=0.57$ )  $\lambda_{osc}$  subsequently jumps to 1529.4 nm. For an Er(1.5 at.%), Yb(11 at.%):YAB crystal, as shown in Fig. 2(b),  $\lambda_{osc}$  versus  $\beta$  curve becomes simpler, where two times significant wavelength jump (from 1609.7 nm to 1603.4 nm and from 1603.4 nm to 1533 nm) can be observed at the critical values of  $\beta=0.19$  and  $\beta=0.48$ .

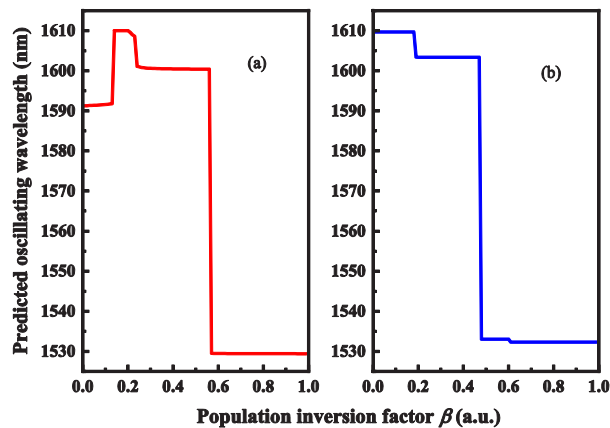


**Fig. 2.** Predicted oscillating wavelength as a function of inversion fraction factor (a) for Er(1.1 at.%), Yb(25 at.%):YAB crystal; (b) for Er(1.5 at.%), Yb(11 at.%):YAB crystal.

Since the critical values of  $\beta$  are invariant when the doped concentration of gain medium and the dispersive behavior of intracavity loss are both fixed. The ETU coefficient ( $C_{ETU}$ ) can be determined by further studying the function relationship between  $\beta$  and  $C_{ETU}$ .

For a CWSFL based on Er,Yb:YAB crystal,  $\beta$  can be defined as

$$\beta = \frac{\iiint_{V_p} N_{2E} dV}{N_E V_p}, \quad (2)$$

where  $N_{2E}$  is the population densities on the  $^4I_{13/2}$  level of  $Er^{3+}$  ions,  $V_p$  is the pump volume inside the crystal.

According to the laser rate equations of Er,Yb:YAB laser at steady state (see Supplement 1),  $N_{2E}$  can be written as a function of  $C_{ETU}$

$$N_{2E} = \frac{-\left\{ \gamma_E + \frac{c\Phi}{n} \sigma_{sum}(\lambda) \phi(r) + \frac{\sigma_Y(\lambda) N_Y}{\alpha N_E} R_p r_p(r, z) \right\} + \sqrt{\left\{ \gamma_E + \frac{c\Phi}{n} \sigma_{sum}(\lambda) \phi(r) + \frac{\sigma_Y(\lambda) N_Y}{\alpha N_E} R_p r_p(r, z) \right\}^2 + 4C_{ETU} \left[ N_E \sigma_{abs}(\lambda) \frac{c\Phi}{n} \phi(r) + \frac{\sigma_Y(\lambda) N_Y}{\alpha} R_p r_p(r, z) \right]}}{2C_{ETU}}, \quad (3)$$

where  $\gamma_E$  is the de-excitation rate of  $Er^{3+}$  ions,  $\sigma_{sum}(\lambda)$  is the sum of  $\sigma_{em}(\lambda)$  and  $\sigma_{abs}(\lambda)$ ,  $c$  is light speed in vacuum.  $k_1$  and  $k_2$  are the coefficients of energy transfer and secondary energy transfer, respectively.  $\sigma_Y(\lambda)$  is the pump absorption cross-section of  $Yb^{3+}$  ions.  $N_Y$  is the population density of  $Yb^{3+}$  ions.  $R_p = P_p(1 - \exp(-\alpha l)) / (h\nu_p)$  and  $r_p(r, z)$  are the pump rate and its distribution function incident on gain medium.  $P_p$  is the pump power incident into gain medium.  $\alpha$  is the pump absorption coefficient of the gain medium.  $l$  is the length of gain medium.  $h\nu_p$  is the pump photon energy.  $r_p(r, z)$  is assumed to be top-hat distribution function that can be read as

$$r_p(r, z) = \frac{\alpha \exp(-\alpha z)}{\pi \omega_{pa}^2 [1 - \exp(-\alpha l)]} \Theta(\omega_{pa}^2 - r), \quad (4)$$

where  $\omega_{pa}$  is the average pump radius in gain medium.  $\Theta()$  is the Heaviside function.

$\Phi = 2P_{out} L_{eff} / [\ln(1/(1-T_{oc}))] ch\nu_0$  is the intracavity laser photon number density,  $P_{out}$  is the output power,  $h\nu_0$  is the laser photon energy.  $\phi(r)$  is its distribution function. Assuming that the oscillation laser is in Gaussian distribution,  $\phi(r)$  can be written as

$$\phi(r, z) = \frac{2}{\pi \omega_0^2 L_{eff}} \exp\left[-\frac{2r^2}{\omega_0^2}\right]. \quad (5)$$

Obviously, if the pump power and emitting laser power at the moment that wavelength jump phenomena occurred are recorded, the value of  $C_{ETU}$  can be determined using Eqs. (2)–(5).

### 3. Experimental setup and results

The schematic of the apparatus for 1.5  $\mu\text{m}$  CWSFL generation and ETU coefficient measurement is depicted in Fig. 3. Two 975 nm polarized pump lights emitted from one laser diode (LD) were shaped by a fiber and re-imaged by a 1.2X telescope system ( $f_1$  and  $f_2$ ) producing a 60  $\mu\text{m}$  diameter focal spot inside the gain medium. The gain medium was an uncoated  $a$ -cut Er,Yb:YAB crystal with different doped concentrations. To reduce the Fresnel reflection and improve the heat dissipation, two 0.8 mm-thick sapphire plates with one facet antireflection coated at 975 nm and 1520 nm~1580 nm were employed and in close contact with the polished facets of the gain

medium. Then the sandwich-scheme gain medium was mounted in a water cooled copper heatsink and maintained at a temperature of 290 K. Single frequency laser operation was guaranteed by unidirectional travelling wave resonator configuration based on an optical diode and an “8” shape ring cavity. The 312 mm-long ring cavity was consisted with 4 concave mirrors ( $M_{1-4}$ ), where the curvature radii of  $M_{1-4}$  were 100 mm, 51.8 mm, 51.8 mm and 100 mm, respectively. Considering the relative low laser gain,  $M_{1-3}$  were all high-reflection coated at  $1.5\ \mu\text{m}$  and high-transmission coated at  $980\ \text{nm}$ , and the output coupler ( $M_4$ ) was coated with a transmittance of 1.2% at  $1.55\ \mu\text{m}$ . During the ETU coefficient measurement, the laser longitudinal mode was monitored utilizing a home-made scanning Fabry-Perot (F-P) interferometer (cavity length: 200 mm, fineness: 260), the pump and emitting laser powers were detected using power meters (PMs, LabMax-TOP, Coherent), the laser wavelength jumps were recorded by a wavelength meter (WM, WS6, High Finesses).

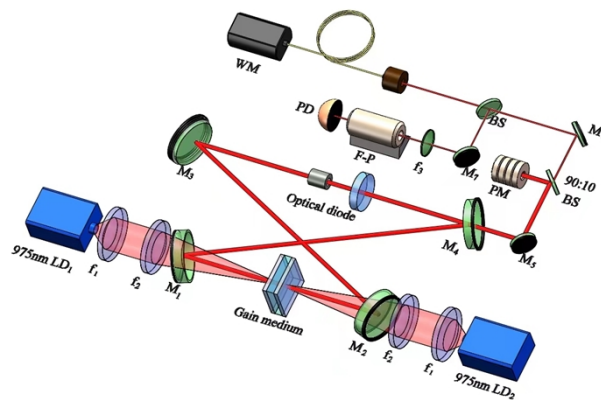


**Fig. 3.** Experimental setup of the  $1.5\ \mu\text{m}$  CWSFL for ETU coefficient measurement. LD<sub>*i*</sub> (*i* = 1,2): laser diode;  $f_j$  (*j* = 1,3): plano-convex lens;  $M_k$  (*k* = 1-4): concave mirror;  $M_k$  (*k* = 5-7): 45° reflector with high reflection coating around  $1.5\sim 1.6\ \mu\text{m}$ ; Gain medium: Er,Yb:YAB crystal; BS: beam splitter; PM: power meter; PD: photodetector; WM: wavelength meter.

When the Er(1.5 at.%),Yb(11 at.%):YAB crystal was adopted as gain medium and temperature controlled at  $10\ ^\circ\text{C}$ , only one time oscillating wavelength jump was observed experimentally. As shown in Fig. 4, the pump and emitting laser powers at the wavelength turning point were respectively 7.77 W and 0.5 W. Then the  $\beta$  versus  $C_{ETU}$  relation can be estimated using Eqs. (2)-(5) and the following parameter values:  $\gamma_E = 3536.2\ \text{s}^{-1}$  [17],  $h\nu_p = 2.038 \times 10^{-19}\ \text{J}$ ,  $\omega_{pa} = 61\ \mu\text{m}$ ,  $\omega_0 = 61\ \mu\text{m}$ ,  $L_{eff} = 312\ \text{mm}$ ,  $l = 1.5\ \text{mm}$ ,  $T_{oc} = 1.2\%$ ,  $\alpha = 12.08\ \text{cm}^{-1}$ , as shown in Fig. 5. Since the  $1.53\ \mu\text{m}$  to  $1.6\ \mu\text{m}$  wavelength jump occurred at  $\beta = 0.48$  according to Fig. 2(a), the value of  $C_{ETU}$  can be determined to be  $5.2 \times 10^{-24}\ \text{m}^3/\text{s}$ . As a comparison,  $C_{ETU}$  of an  $\text{Er}^{3+}$  and  $\text{Yb}^{3+}$  codoped phosphate glass is typically  $1 \times 10^{-24}\ \text{m}^3/\text{s}$  [18], while that of Er,Yb:YCOB and Er,Yb:YAG are  $13 \times 10^{-24}\ \text{m}^3/\text{s}$  and  $2.5 \times 10^{-24}\ \text{m}^3/\text{s}$  [19]. One can find that ETU process is relatively stronger in borate crystal based gain media with respect to gain media based on other substrates.

Considering the uniqueness of the functional relationship between laser wavelength evolution and pump powers at a specific ETU strength, the value of ETU coefficient can be evaluated by fitting the experimental data with the procedure similar to Figs. 4 and 5. It is well known that the spectroscopic parameters of a laser crystal are all temperature and doped concentration dependent, experiment and theoretical fittings mentioned above were performed repeatedly at different heatsink temperature, as well as different crystal doped concentrations. Figure 6 shows the measured ETU coefficient versus heatsink temperature at two cases. Curve i and red blocks in Fig. 6(a) indicates the averaged value of ETU coefficient of a Er,Yb:YAB crystal with a  $\text{Er}^{3+}$  doped concentration of 1.5 at.% and a  $\text{Yb}^{3+}$  doped concentration of 11 at.% during 10

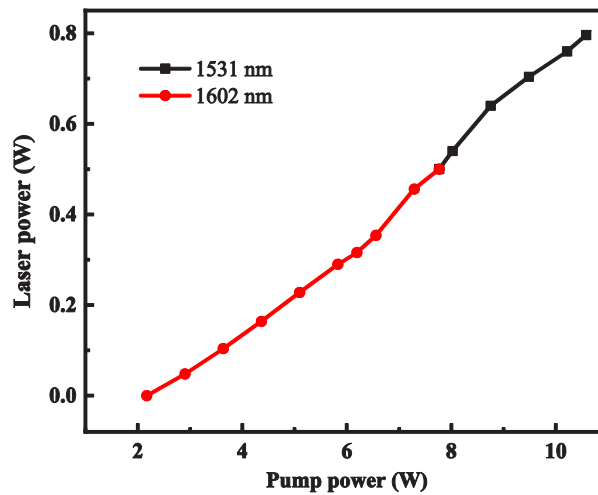


**Fig. 4.** Input-output behavior of Er(1.5 at.%), Yb(11 at.%):YAB laser operating at 10 °C.

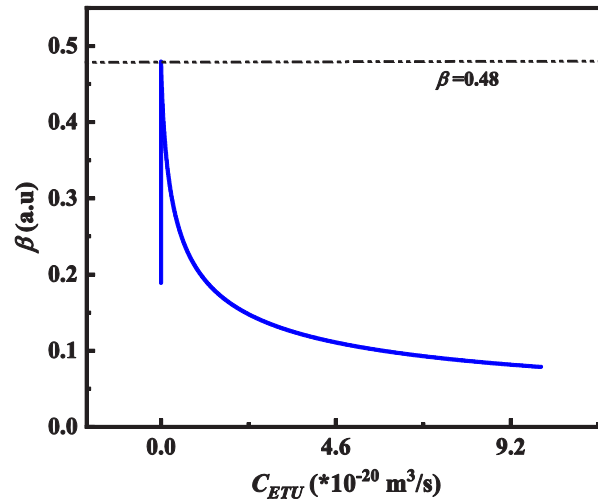


**Fig. 5.** Estimated critical value of  $\beta$  as a function of  $C_{etu}$  and the experimental data.

independent measurements, curve ii and blue balls in Fig. 6(b) indicates the averaged value of ETU coefficient of a Er,Yb:YAB crystal with a  $\text{Er}^{3+}$  doped concentration of 1.1 at.% and a  $\text{Yb}^{3+}$  doped concentration of 25 at.% during 10 independent measurements, while the error bars correspond to the standard deviations in repeated measurements. It can be seen, for the low doped crystal,  $C_{ETU}$  increases from  $5.2*10^{-24} \text{ m}^3/\text{s}$  to  $24.6*10^{-24} \text{ m}^3/\text{s}$  monotonically with increasing heatsink temperature varied in the range from 10 °C to 40°C. Apparently,  $C_{ETU}$  of Er,Yb:YAB is quite higher than that of  $\text{Er}^{3+}$  and  $\text{Yb}^{3+}$  codoped phosphate glass, and is significantly dependent on the crystal temperature. Since ETU strength is related to the population density in excited states,  $C_{ETU}$  should be even higher for the high doped crystals. For Er(1.1 at.%), Yb(25 at.%):YAB crystal,  $C_{ETU}$  at specific temperature shows nearly 3.2-fold increase with respect to the Er(1.5 at.%), Yb(11 at.%):YAB crystal, while the value of  $C_{ETU}$  ranges from  $15.7*10^{-24} \text{ m}^3/\text{s}$  to  $36.6*10^{-24} \text{ m}^3/\text{s}$  during temperature variation.

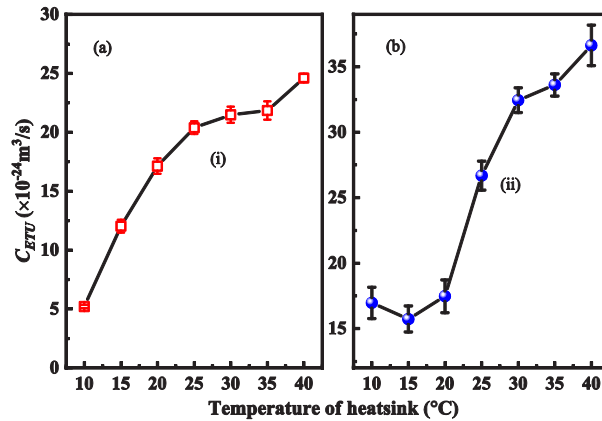


**Fig. 6.** Measured ETU coefficient as a function of heatsink temperature at two cases. (i) doped concentration for  $\text{Er}^{3+}$  and  $\text{Yb}^{3+}$  were 1.5 at.% and 11 at.%; (ii) doped concentration for  $\text{Er}^{3+}$  and  $\text{Yb}^{3+}$  were 1.1 at.% and 25 at.%.

Nevertheless, it should be noted that the influence of excited state absorption (ESA) effect on the population density in the upper laser level was neglected since the measured ESA spectra of Er,Yb:YAB did not overlap with the stimulated emission band [26]. When the method is transferred to other similar laser systems, and there exists an overlap between the ESA and stimulated emission spectra, the ESA cross-section ( $\sigma_{esa}$ ) spectra need to be measured before theoretical simulations, and the stimulated emission cross-section ( $\sigma_e$ ) in all the equations should be replaced by  $\sigma_e - \sigma_{esa}$ . Besides that, the laser should be operated in single mode, otherwise multi-wavelength laser radiation that disturbs the determination of wavelength jumping may take place. Moreover, due to the relative high laser threshold, only one time wavelength jumping was observed in our measurements. When the output coupling transmission is low enough, two or more times wavelength jumping may be detected in each measurement, then the accuracy of the determination of the ETU coefficient can be further improved by averaging the simulated values obtained at the two wavelength jumping points.

#### 4. Conclusion

In summary, we proposed a novel method of ETU coefficient estimation for some special laser systems, for instance that based on  $\text{Er}^{3+}$  doped,  $\text{Ho}^{3+}$  doped,  $\text{Er}^{3+}$  and  $\text{Yb}^{3+}$  codoped gain media, etc, getting over the difficulties stemmed from the wavelength jump phenomena. The core of the method was a theoretical model that establishing the association between the inversion fraction factor and the emitting laser wavelength, as well as that between the inversion fraction factor and the ETU coefficient. Based on this model, ETU coefficients and their temperature dependences of Er,Yb:YAB crystals with different crystal doped concentrations were experimentally determined for the first time. The results show that the ETU process in Er,Yb:YAB laser system is much stronger than that in  $\text{Er}^{3+}$  and  $\text{Yb}^{3+}$  codoped phosphate glass. The determination of these spectroscopic data provides the prospect to precise modelling of laser system based on Er,Yb:YAB or any other similar gain media, which has been rarely seen up to date.

**Funding.** National Natural Science Foundation of China (62175135, 61405109); Special Foundation of Local Scientific and Technological Development Guided by Central Government (YDZJSX20231A006); Fundamental Research Program of Shanxi Province (202103021224025).

**Disclosures.** The authors declare no conflicts of interest.

**Data availability.** Data underlying the results presented in this paper are not publicly available at this time but may be obtained from the authors upon reasonable request.

**Supplemental document.** See [Supplement 1](#) for supporting content.

## References

1. R. Scheps, "Upconversion laser processes," *Prog. Quantum Electron.* **20**(4), 271–358 (1996).
2. J. W. Kim, J. I. Mackenzie, and W. A. Clarkson, "Influence of energy-transfer-upconversion on threshold pump power in quasi-three-level solid state lasers," *Opt. Express* **17**(14), 11935–11943 (2009).
3. Y. Ma, Y. Li, J. Feng, *et al.*, "Influence of energy-transfer upconversion and excited-state absorption on a high power Nd:YVO<sub>4</sub> laser at 1.34 μm," *Opt. Express* **26**(9), 12106–12120 (2018).
4. S. Cante and J. I. M. Mackenzie, "Energy transfer upconversion in Nd:YAG at cryogenic temperatures," *Opt. Mater. Express* **10**(9), 2019–2029 (2020).
5. S. Bjurshagen and R. Koch, "Modeling of energy-transfer upconversion and thermal effects in end-pumped quasi-three-level lasers," *Appl. Opt.* **43**(24), 4753–4767 (2004).
6. T. Förster, "Intermolecular energy migration and fluorescence," *Annal. Phys.* **2**, 55–75 (1948).
7. D. L. Dexter, "A theory of sensitized luminescence in solids," *J. Chem. Phys.* **21**(5), 836–850 (1953).
8. N. P. Barnes, B. M. Walsh, F. Amzajerdian, *et al.*, "Up conversion measurements in Er:YAG; comparison with 1.6 μm laser performance," *Opt. Mater. Express* **1**(4), 678–685 (2011).
9. G. C. Jones and S. N. Houde-Walter, "Determination of the macroscopic upconversion parameter in Er<sup>3+</sup>-doped transparent glass ceramics," *J. Opt. Soc. Am. B* **23**(8), 1600–1608 (2006).
10. W. J. Lima, V. M. Martins, A. F. G. Monte, *et al.*, "Energy transfer upconversion on neodymium doped phosphate glasses investigated by Z-scan technique," *Opt. Mater. Express* **35**(9), 1724–1727 (2013).
11. W. R. Kerridge-Johns and M. J. Damzen, "Temperature effects on tunable cw alexandrite lasers under diode end-pumping," *Opt. Express* **26**(6), 7771–7785 (2018).
12. S. Y. Feng, F. Luan, S. G. Li, *et al.*, "Determination of energy transfer and upconversion constants for Yb<sup>3+</sup>/Er<sup>3+</sup> codoped phosphate glass," *Chin. Opt. Lett.* **8**(2), 190–193 (2010).
13. J. W. Kim, I. O. Musgrave, M. J. Yarrow, *et al.*, "Simple technique for measuring the energy-transfer-upconversion parameter in solid-state laser materials," in *CLEO/Europe and IQEC 2007 Conference Digest* (Optical Society of America, 2007), paper CA\_40.
14. N. F. Zhuang, X. L. Hu, S. K. Gao, *et al.*, "Spectral properties and energy transfer of Yb,Er:GdVO<sub>4</sub> crystal," *Appl. Phys. B* **82**(4), 607–613 (2006).
15. S. Taccheo, G. Sorbello, S. Longhi, *et al.*, "Measurement of the energy transfer and up-conversion constants in Er-Yb-doped phosphate glass," *Opt. Quantum Electron.* **31**(3), 249–262 (1999).
16. T. Y. Fan, G. Huber, R. L. Byer, *et al.*, "Spectroscopy and diode laser-pumped operation of Tm,Ho:YAG," *IEEE J. Quantum Electron.* **24**(6), 924–933 (1988).
17. W. X. You, Y. F. Lin, Y. J. Chen, *et al.*, "Polarized spectroscopy of Er<sup>3+</sup> ions in YAl<sub>3</sub>(BO<sub>3</sub>)<sub>4</sub> crystal," *Opt. Mater.* **29**(5), 488–493 (2007).
18. B. C. Hwang, S. Jiang, T. Luo, *et al.*, "Cooperative upconversion and energy transfer of new high Er<sup>3+</sup> and Yb<sup>3+</sup>-Er<sup>3+</sup> doped phosphate glasses," *J. Opt. Soc. Am. B* **17**(5), 833 (2000).
19. P. A. Burns, J. M. Dawes, P. Dekker, *et al.*, "Optimization of Er,Yb:YCOB for CW laser operation," *IEEE J. Quantum Electron.* **40**(11), 1575–1582 (2004).
20. Z. J. Yao, Y. J. Li, K. L. Liu, *et al.*, "Wavelength tuning of solid-state-continuous-wave single frequency 1.5 μm laser by manipulating net gain spectra," *Opt. Express* **30**(24), 44085–44094 (2022).
21. Y. Zhang, B. Chen, Y. Cao, *et al.*, "High-color-rendering white light and broadband optical gain of Ag-aggregates/Mn<sup>2+</sup> co-doped germanate glasses," *J. Non-Cryst. Solids* **596**, 121851 (2022).
22. N. A. Tolstik, S. V. Kurilchik, V. E. Kisel, *et al.*, "Efficient 1 W continuous-wave diode-pumped Er,Yb:YAl<sub>3</sub>(BO<sub>3</sub>)<sub>4</sub> laser," *Opt. Lett.* **32**(22), 3233–3235 (2007).
23. Y. J. Chen, Y. F. Lin, X. H. Gong, *et al.*, "2.0 W diode-pumped Er:Yb:YAl<sub>3</sub>(BO<sub>3</sub>)<sub>4</sub> laser at 1.5–1.6 μm," *Appl. Phys. Lett.* **89**(24), 241111 (2006).
24. X. Mateos, S. Lamrini, K. Scholle, *et al.*, "Holmium thin-disk laser based on Ho:KY(WO<sub>4</sub>)<sub>2</sub>/KY(WO<sub>4</sub>)<sub>2</sub> epitaxy with 60% slope efficiency and simplified pump geometry," *Opt. Lett.* **42**(17), 3490–3493 (2017).
25. X. Sha, B. Chen, X. Zhang, *et al.*, "Pre-assessments of optical transition, gain performance and temperature sensing of Er<sup>3+</sup> in NaLn(MoO<sub>4</sub>)<sub>2</sub> (Ln = Y, La, Gd and Lu) single crystals by using their powder-formed samples derived from traditional solid state reaction," *Opt. Laser Technol.* **140**, 107012 (2021).